

# Bacterium in a box: sensing of quorum and environment by the *LuxI/LuxR* gene regulatory circuit

Stephen J. Hagen · Minjun Son · Joel T. Weiss · Jonathan H. Young

Received: 10 November 2009 / Accepted: 18 January 2010 /  
Published online: 10 February 2010  
© Springer Science+Business Media B.V. 2010

**Abstract** The chemical signaling mechanism known as “bacterial quorum sensing” (QS) is normally interpreted as allowing bacteria to detect their own population density, in order to coordinate gene expression across a colony. However, the release of the chemical signal can also be interpreted as a means for one or a few cells to probe the local physical properties of their microenvironment. We have studied the behavior of the *LuxI/LuxR* QS circuit of *Vibrio fischeri* in tightly confining environments where individual cells detect their own released signals. We find that the *lux* genes become activated in these environments, although the activation onset time shows substantial cell-to-cell variability and little sensitivity to the confining volume. Our data suggest that noise in gene expression could significantly impact the utility of *LuxI/LuxR* as a probe of the local physical environment.

**Keywords** Quorum sensing · Noise · Microenvironments · Fluorescence · GFP · Diffusion · Bacteria · *LuxI* · *LuxR* · Stochastic · Bioluminescence · Autoinduction · *Vibrio fischeri*

## 1 Introduction

Many bacterial species regulate important behaviors through a chemical signaling mechanism known as “quorum sensing” (QS) [1]. Individual cells release small molecules, known as “autoinducers” (AI), into their local environment while also responding to the local concentration of the same molecule. A density of bacteria sufficient to raise the local concentration of AI above a threshold then triggers changes in gene expression throughout the population. Hence, QS allows the population density of the microbes to control or synchronize gene expression within individual cells. Quorum sensing occurs in numerous Gram-negative and Gram-positive species, where it may regulate such diverse functions as

---

S. J. Hagen (✉) · M. Son · J. T. Weiss · J. H. Young  
Physics Department, University of Florida, PO Box 118440, Gainesville, FL 32611-8440, USA  
e-mail: sjhagen@ufl.edu

bioluminescence, genetic competence, surface attachment, biofilm formation, secretion of toxins or proteases, and other forms of virulence. These functions presumably provide maximum benefit to the individual bacterium if other members of the colony act in synchrony.

It is increasingly clear, however, that the function of a QS pathway goes beyond simple population counting. For example, many bacteria produce several chemically distinct AI, secrete AI at a rate that is subject to feedback control, or even actively degrade AI signal [2, 3]. These behaviors would probably not be necessary if QS functioned solely to count population density. Some authors have observed that interpreting QS as a mechanism of intercellular cooperation raises difficult questions of evolution and may not be strictly necessary in all instances [4, 5]: An individual cell may derive direct benefits from producing, releasing, and detecting AI if this activity provides useful information about the immediate environment of the cell. For example, the secretion of an exoenzyme best serves the bacterium if the enzyme and its digestive products remain physically near to the organism. In this case, releasing a small molecule AI into the environment may act as a useful probe of local diffusion or advection, prior to releasing enzymes that are more costly to synthesize. A high concentration of AI in the vicinity of a microbe could also signal a clustered spatial distribution of cells, or confinement to a small volume, rather than overall population density [4]. Thus, a single cell confined within a small chamber could conceivably read the concentration of its AI as a clue to the volume of its confining environment. Thus, one may argue that QS does not measure population density as much as it measures the efficiency of local diffusion and mixing [4, 5]. The question of whether QS is really “diffusion sensing” (DS) raises questions of exactly what information the cell can obtain about its environment through a QS mechanism, and how this information changes in different physical environments. To begin to distinguish between QS and DS, we need to examine how the QS mechanisms of individual cells respond to distinctly different physical microenvironments.

The bioluminescence of the marine bacterium *Vibrio fischeri* is one of the best-known examples of QS-regulated behavior [1, 6]. The AinR/AinS and LuxI/LuxR QS systems of *V. fischeri* both use acyl homoserine lactone (HSL) AI to regulate the activity of the *lux* genes, which are responsible for production of the luciferase that generates bioluminescence [1, 6, 7]. The LuxI/LuxR system has been subject to the most extensive study. It is a positive-feedback circuit that includes an AI synthase LuxI and a transcriptional activator LuxR, which binds or detects the AI *N*-(3-oxohexanoyl)-L-HSL (3-oxo-C6 HSL) to activate the *lux* genes. At high cell densities, where 3-oxo-C6 HSL is abundant, the *lux* genes are activated, producing LuxI and LuxR as well as the bacterial luciferase and related enzymes. At low cell densities, the *lux* genes are not expressed and luminescence is absent. Hence, the LuxI/LuxR system serves as a population-sensitive switch that not only serves *V. fischeri* in its natural symbiotic niche [6] but can also be artificially engineered into other organisms to control a wide range of cellular processes such as cell death [8] and recombinant gene expression [9].

Although a number of modeling studies have examined the dynamics and stochasticity of LuxI/LuxR circuit models at the level of individual cells [10–12], there are few experimental studies of LuxI/LuxR in single cells or small clusters. We have studied the response of the LuxI/LuxR system to physical confinement of individual cells, which can detect their own AI but are isolated from any larger population. By trapping individual cells containing LuxI/LuxR within small, closed chambers of picoliter volume, we can ask whether the QS circuit responds to a cell’s own AI and whether this response may contain information of potential value to the cell.

## 2 Methods

We fabricated an array of micron-sized chambers from a soft silicone polymer (polydimethylsiloxane [PDMS]), using soft-lithographic techniques [13] at the Nanoscale Research Facility of the University of Florida. A rectangular pattern of  $\sim 15 \times 15$ - or  $30 \times 30$ - $\mu\text{m}^2$  squares on a transparency mask is imaged onto a silicon wafer that is coated with a thin layer of AZ9260 positive photoresist (MicroChemicals GmbH). Development of the photoresist then leaves an array of small photoresist posts rising from the silicon surface. Transparent PDMS elastomer (Sylgard 184; Dow Corning Inc.) is then poured over the silicon wafer. After several hours at  $60$ – $70^\circ\text{C}$ , the elastomer cures to a solid and can be pulled away from the silicon. The array pattern then appears as shallow wells or chambers ( $\sim 16$ – $17$   $\mu\text{m}$  deep) in the surface of the PDMS. When sealed with a coverslip, the final volume of the chambers was typically  $3.4 \pm 0.6$  pl for the smaller chambers and  $18.4 \pm 2.6$  pl for the larger chambers.

*Vibrio fischeri* strain MJ11 was provided by Dr. Mark Mandel and Dr. Ned Ruby. *Vibrio fischeri* was grown to a population density of  $\sim 1.5 \times 10^8$  cells/ $\text{cm}^3$  in photobacterium complete broth (Carolina Biological Supply Co.) at  $25^\circ\text{C}$  on an orbital shaker. At this stage of growth, the cells were not luminescent. A sample of 1 ml was then extracted, and any AI present was removed by three cycles of washing: Each cycle consisted of microcentrifugation, replacement of the supernatant by a fresh growth medium, and resuspension of the cells. Each cycle should have reduced any initial AI (3-oxo-C6 HSL) concentration by a factor of at least  $\sim 20\times$ , so that these washes would have reduced any AI concentration by a factor of at least  $8,000\times$ . Both the removal of the AI and the presence of a consumable inhibitor in fresh complete medium (the so-called rich medium effect) act to suppress the luminescence of *V. fischeri* that has been washed in the fresh complete medium [14]. A sample of 5–6  $\mu\text{l}$  of the culture was then spread over the PDMS microarray and sealed with a 25-mm square coverslip. The microarray was placed on a microscope stage and imaged in phase contrast (Nikon TE2000-U inverted microscope with  $20\times$  plan fluor objective, NA 0.5) until a few chambers containing individual cells were found. Cells were observed to be trapped within the chambers and swimming, and continued swimming vigorously for many hours. We then imaged these cells on a charge-coupled device (CCD) camera using a  $60\times$  plan apo NA 1.4 oil immersion objective, in order to collect bioluminescence light. The detector was a MicroMax CCD camera ( $1,300 \times 1,030$  array of  $6.7$ - $\mu\text{m}$  pixels with 12-bit readout, Princeton Instruments, Inc.) cooled to  $-15^\circ\text{C}$  or  $-20^\circ\text{C}$ , with typically 10-min exposures.

*Escherichia coli* MC1061 harboring the plasmid pAC-LuxGfp [15] was provided by Dr. Rena Hill and Dr. Christopher Voigt. This strain contains LuxI/LuxR, produces and detects the AI 3-oxo-C6 HSL, and produces green fluorescent protein (GFP) upon activation of the LuxI/LuxR circuit. Exponential-phase cells were grown at  $37^\circ\text{C}$  in a Luria-Bertani (LB) medium with  $34$ - $\mu\text{g}/\text{ml}$  chloramphenicol on an orbital shaker. When the population density reached  $\sim 2 \times 10^7$  cells/ $\text{cm}^3$  (i.e., before activation of LuxI/LuxR and expression of *gfp*), we extracted 1 ml of culture and washed the cells to remove any AI that may have already been produced. The cells were washed by 2–3 cycles of microcentrifugation, replacement of the supernatant by a fresh LB medium, and resuspension of the cells. Any initial AI concentration would then have been diluted by at least  $400\times$  to  $8,000\times$  before the cells were loaded into the chambers. We then spread 5–6  $\mu\text{l}$  of the washed cell suspension onto the surface of the PDMS microarray and sealed it with a 25-mm square coverslip. In the control experiment with exogenous AI, the cells grew in an LB medium containing

34- $\mu\text{g/ml}$  chloramphenicol and 1- $\mu\text{M}$  added AI [*N*-(3-oxohexanoyl)-L-HSL, CAS 143537-62-6, Sigma-Aldrich K3007]. The cells were then washed as above in a fresh LB medium that contained the 1- $\mu\text{M}$  added AI.

Examination of the array in phase contrast revealed many individual chambers containing one or two live, actively swimming *E. coli* cells. With the coverslip sealed firmly against the PDMS surface to prevent evaporation of the medium, the cells remained alive and swimming for many hours at room temperature. We located a region of the microarray in which few, if any, chambers appeared to contain more than one cell. We then imaged this region in GFP fluorescence at 20 $\times$ . With a 0.7 $\times$  camera adapter and a 20 $\times$  objective, each CCD pixel images an area of  $0.48 \times 0.48 \mu\text{m}^2$ . By collecting a series of images at 25 $^\circ\text{C}$ , with 3–10-s exposures, over a period of hours, we could detect the onset of GFP fluorescence.

To quantify the GFP fluorescence of each chamber, we determined the mean and standard deviation of the baseline image intensity as observed in the dark regions between neighboring chambers. Setting a threshold at a level 2 or 3 standard deviations above the mean background intensity, we summed the intensities of those pixels that lay within the area of a particular chamber and that exceeded the threshold. This method sums the GFP fluorescence of all cells residing within that chamber and gives results that are relatively insensitive to the choice of threshold level.

### 3 Results

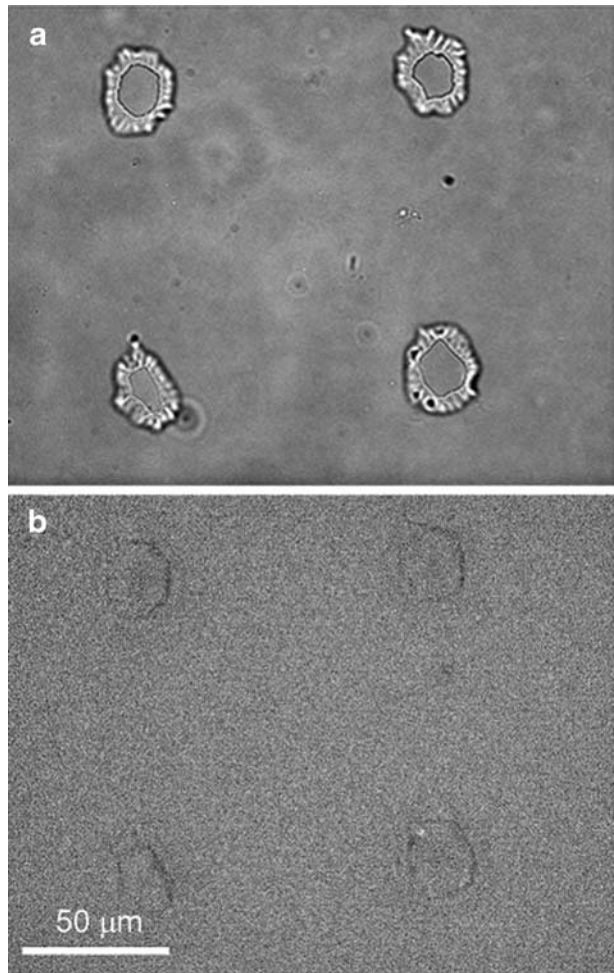
Individual cells of *V. fischeri* confined to microscopic chambers of  $3.4 \pm 0.6$ -pl volume continued actively dividing and swimming vigorously for a period of at least 6 h at 25 $^\circ\text{C}$ . The near-constant motion of the cells, together with the short depth of field of the 60 $\times$  NA 1.4 objective, spreads the collected bioluminescence over many sensor pixels and makes it difficult to detect that light above the dark current in the CCD. However, some cells occasionally lodge themselves temporarily into a position reasonably close to the focal plane, allowing the camera to detect a luminescence signal. Figure 1 shows four chambers, where a cell within the lower right chamber is seen to exhibit some luminescence after  $\sim 4.5$  h of confinement. This confirms that the luminescence of *V. fischeri* MJ11 can be induced by confining the bacterium within a micron-sized chamber.

However, bioluminescence clearly produces a weak experimental signal, which precludes quantitative analysis of autoinduction in single cells. For this reason, we repeated the experiment using *E. coli* harboring the plasmid pAC-LuxGfp, a synthetic LuxI/LuxR system that produces and detects the AI (3-oxo-C6 HSL) and expresses GFP rather than luciferase upon induction [15]. Because GFP fluorescence is far brighter than *V. fischeri* luminescence, it is far easier to quantify autoinduction of LuxI/LuxR in the *E. coli* mutant, especially in small numbers of motile cells.

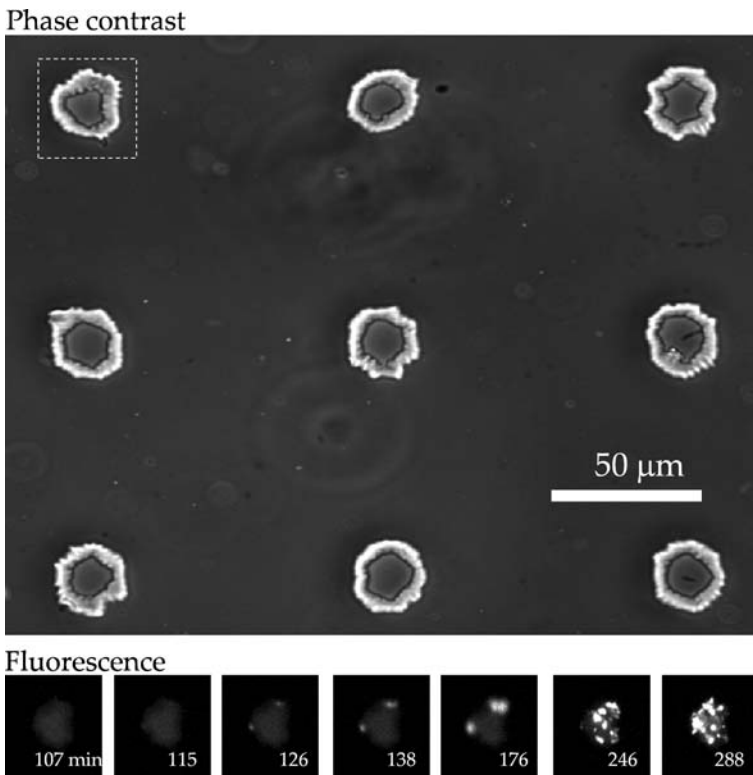
We found that this *luxI/luxR-gfp* strain of *E. coli* initiates *gfp* expression when confined to within a micron-sized chamber. Figure 2 shows fluorescence images collected at various times following trapping of cell within a chamber of volume of  $\sim 3$  pl. The chamber remains dark until  $\sim 120$  min, when fluorescence switches on fairly abruptly. At longer times, the number of cells in the chamber increases markedly as the overall fluorescence increases.

Figure 3 shows the magnitude of the fluorescence signal collected from several 3-pl chambers, as a function of time after insertion of the live cells. Some background

**Fig. 1** **a** Phase-contrast image of four microarray chambers, each roughly 3  $\mu\text{l}$  in volume. The upper left chamber and both lower chambers initially contained a single *V. fischeri* cell. The upper right chamber remained empty. The irregular light and dark patterns surrounding each chamber are features of the PDMS walls; the live cells are not readily visible in this image. **b** Luminescence image of the same chambers after 4.5 h. A region of bioluminescence is visible in the lower right chamber, signaling activation of the *lux* genes



fluorescence is observed from the LB growth medium, even in the absence of any live cells. The fluorescence remains at this background level for the first 1–1.5 h. During this time, the cells divide with a generation time of roughly 1.5 h. At  $\sim 100$ –200 min, however, the emission rises steeply in those chambers that contain cells, indicating autoactivation of the QS circuit. The time at which GFP appears varies noticeably from one chamber to the next. The “onset time,” which we define as the time at which the fluorescence level exceeds the background fluorescence by tenfold, ranges from 116 to 210 min in the six chambers that become activated in Fig. 3. Chambers that contained no cells show no rise in signal at this time. However, after a few hours, all chambers that do contain cells eventually attain a comparable level of *gfp* fluorescence intensity. Although the cells divide during the experiment, the population in each (occupied) chamber remains similar from one chamber to another. The cells remain alive for the duration of the experiment, with numerous brightly fluorescent and swimming cells visible in the occupied chambers after 4–6 h.



**Fig. 2** *Upper*: Phase-contrast image of nine chambers (volume  $3.4 \pm 0.6$  pl) containing pAC-LuxGfp *E. coli*. Cells appear as dark rodlike shapes near the centers of the two lower chambers in the *right hand column*. The *white box* indicates the chamber whose fluorescence is imaged in the *lower panel*. *Lower*: GFP fluorescence images for the chamber indicated above, collected at various times (with 10-s exposures) after trapping of a single cell. The LB medium gives a weak fluorescent background, but the abrupt onset of GFP fluorescence is apparent at  $\sim 120$  min

**Fig. 3** Fluorescence versus time for microarray chambers of  $\sim 3$ -pl volume, loaded with pAC-LuxGfp *E. coli*. Each *curve* represents a single chamber. Cells were loaded at time zero. Most chambers that did capture cells eventually attain similar fluorescence intensity, near  $\sim 10^5$  counts. However, many chambers contain no cell at the start of the experiment; their fluorescence remains near background levels ( $10$ – $10^2$  counts)

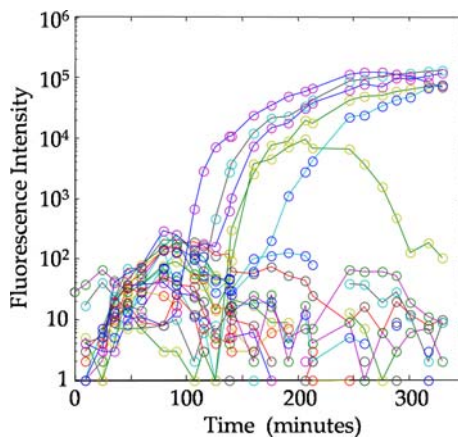
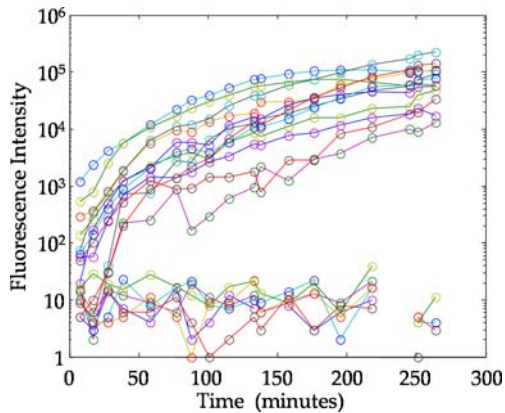




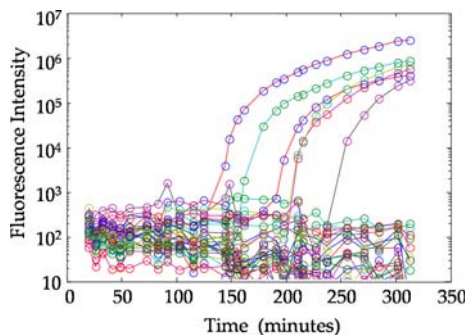
**Fig. 4** Fluorescence versus time for individual  $\sim 3$ -pl microarray chambers loaded with pAC-LuxGfp *E. coli* with AI added. Live cells were incubated and washed in a growth medium containing  $1\text{-}\mu\text{M}$  exogenous AI, prior to trapping in the microarray. Some chambers contain no cells



We could not measure the concentration of the AI produced within the chambers. We did, however, perform a control experiment to verify that the abrupt onset of GFP fluorescence is due to the need for the cells to accumulate AI. Figure 4 shows an experiment where the cells are first grown in a medium containing  $1\text{-}\mu\text{M}$  AI, which is sufficient to saturate the LuxI/LuxR pathway. The cells were washed twice in a fresh medium also containing  $1\text{ }\mu\text{M}$  AI and then inserted into the device. The GFP signal in this case shows very different kinetics than in Figs. 2 and 3: the fluorescence from each (nonempty) chamber grows steadily with time, rather than switching on abruptly. The steady growth of the fluorescence signal in the images over the duration of the experiment ( $>4$  h) is consistent with the steady and continuous production and accumulation of GFP by a LuxI/LuxR circuit that is switched on by a saturating concentration of AI. This control experiment verifies that the  $\sim 100$ – $200$ -min delay in the onset of GFP expression in Fig. 3 results from the initial lack of AI.

Finally, Fig. 5 shows an experiment performed with LuxI/LuxR *E. coli* confined within larger chambers, of  $18.4 \pm 2.6$ -pl volume. As in the 3-pl chambers, the fluorescence remains at background levels for more than 1 h and then rises abruptly in those chambers that contain cells. Again, the onset time varies substantially between chambers, spanning a range from  $\sim 150$ – $250$  min in the six chambers that contained cells. Although the cells require a longer time to activate the LuxI/LuxR circuit in the larger chambers, the onset time does not scale in proportion to the chamber volume (see below).

**Fig. 5** Fluorescence versus time for microarray chambers of volume  $18.4 \pm 2.6$  pl, loaded with pAC-LuxGfp *E. coli*. Each curve represents a single chamber. The LB medium contributes a background fluorescence of roughly  $10^2$ – $10^3$  counts per chamber



## 4 Discussion

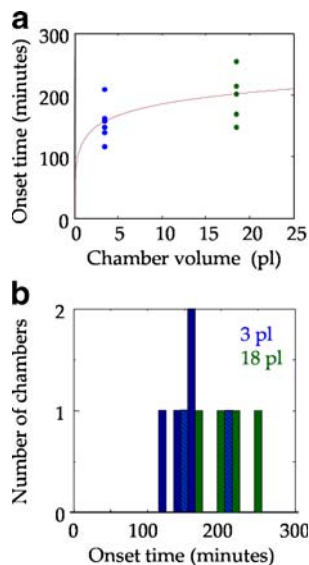
Figure 1 shows that confining MJ11 *V. fischeri* to a sufficiently small volume can trigger activation of the *lux* genes. However, activation in a volume of  $\sim 3$  pl was only weakly detectable after  $\sim 4.5$  h, owing largely to the motility of the cells and their faint bioluminescence. For this reason, we repeated the experiment with *E. coli* containing a *luxI/luxR-gfp* QS system, which generates a bright GFP fluorescence signal upon autoinduction.

When trapped inside the chambers, the LuxI/LuxR strain of *E. coli* produced a strong autoinduction signal within 2–3 h: The time required for onset of detectable autoinduction of *gfp* expression was  $156 \pm 31$  min (mean  $\pm$  standard deviation) in the 3.4-pl chambers and  $201 \pm 38$  min in the 18-pl chambers (Fig. 6). Since the doubling time of this strain was measured at  $\sim 90$  min in this medium at  $25^\circ\text{C}$ , it appears that cells have typically divided one or two times before autoinduction (Fig. 2).

The broad distribution of onset times is remarkable: For chambers of both sizes, the longest onset time exceeds the shortest time by  $\sim 70$ – $80\%$ . We note that a very recent study of QS in *Pseudomonas aeruginosa* also found variability in the onset of QS in small clusters confined in microwells, with some cells evidently not initiating QS in this environment [16]. In our experiment, by contrast, all chambers that contained visible cells eventually displayed an onset of QS. A very recent study of *Staphylococcus aureus* also showed nearly complete QS [17].

For our *E. coli* data, the magnitude of the cell-to-cell differences in onset time raises the question of whether the same number of viable cells was initially trapped in each chamber. Initial inspection under phase contrast only suggested—but could not prove—that no chamber (in the selected region of the microarray) contained more than one cell at the start of the experiment. Cells adhering to the chamber walls and not visibly swimming were difficult to observe in the chambers, and if present, they would alter the chamber's initial state and thereby broaden the distribution of onset times.

**Fig. 6** **a** Measured onset times for autoinduction of pAC-LuxGfp *E. coli*, versus chamber volume. Dotted curve shows fit to Eq. 2 with  $\tau \approx 27 \pm 10$  min and  $C^*/k \sim 2,600 \pm 3,800$  min/pl. **b** Histogram of onset times for smaller (blue) and larger (green) chambers





However, a statistical argument suggests that this is unlikely. Of the 27 chambers tracked in Fig. 5, six chambers showed GFP fluorescence (indicating the presence of live cells) by the end of the experiment. The other 21 chambers appeared empty throughout the measurement. Thus, a majority ( $21/27 = 78\%$ ) of the chambers were empty. If  $m$  represents the average number of cells trapped per chamber at the start of the experiment, the probability of a chamber trapping  $n$  cells should be given by the Poisson distribution,

$$P(n, m) = m^n \exp(-m)/n! \quad (1)$$

We estimate the value of  $m$  as being that value that gives the probability of an empty chamber ( $n = 0$ ) as  $P(0, m) = 21/27$ , or  $m = \log(27/21) = 0.248$ . Therefore, the average chamber trapped  $\sim 0.25$  cells. In this case, Eq. 1 predicts that 97% of the chambers would have trapped fewer than two cells, and 99.8% would have trapped fewer than three cells. Similarly, in the data of Fig. 3, 12 out of 18 chambers were dark throughout the experiment. This suggests that an average  $m = \log(18/12) = 0.41$  cells were initially trapped in each chamber, so that 94% of the chambers would have trapped fewer than two cells.

These estimates imply that most of the chambers that became fluorescent in Figs. 3 and 5 were likely to have started with one trapped cell. Then, the observed distribution in the time for autoinduction should reflect variability in the efficiency of self-activation of the LuxI/LuxR circuit, rather than in the initial number of cells. One potential origin for this difference in the rate of autoinduction is a statistical fluctuation in the initial number of LuxI (AI synthase) molecules present. (The magnitude of fluctuation exceeds the relative variation anticipated for the plasmid copy number.) An average of 10–20 LuxI molecules would lead to fluctuations of order  $1/\sqrt{10}$  or  $1/\sqrt{20}$ , i.e., differences of 20–30% in the AI synthesis rate and (consequently) in the onset time for QS.

In fact, Fig. 6 shows that the variation between individual cells has a larger effect on the rate of autoinduction than does the volume of the chamber. The average autoinduction time increases only  $\sim 30\%$  when the volume of the chambers increases by  $\sim 5\times$ . This is not surprising if, on the time scale of autoinduction, the cells undergo exponential growth. Then, the rate of AI production increases (roughly) exponentially with time. With the total number of AI molecules increasing exponentially in  $t$ , the time  $t^*$  required to reach a triggering threshold may only grow logarithmically with the volume of the chamber.

We can demonstrate this behavior with a simple model where the number  $N$  of AI molecules in the chamber begins at  $N = 0$  and then increases at a rate proportional to the number  $n$  of cells in the chamber,

$$dN/dt = kn$$

where  $k$  (molecules/min/cell) is the basal production rate of AI. (This model ignores stochasticity in the synthesis and detection of AI.) In exponential growth, the number of cells  $n$  in the chamber grows exponentially with time  $t$

$$n = \exp(t/\tau)$$

where  $\tau = (\text{cell division time})/\log(2)$ . Then, the concentration  $C$  of AI molecules in a chamber of volume  $V$  grows as

$$dC/dt = (k/V) \exp(t/\tau),$$

or

$$C(t) = (k\tau/V) (\exp(t/\tau))^{-1}.$$

The AI concentration reaches an autoinduction threshold  $C^*$  at a time

$$t^* = \tau \log(1 + VC^*/k\tau) \quad (2)$$

that varies logarithmically with  $V$ , as expected. Figure 6 shows a fit to Eq. 2, which gives  $\tau \approx 27 \pm 10$  min and  $C^*/k \sim 2,600 \pm 3,800$  min/pl. Although this growth time  $\tau$  is somewhat too fast for *E. coli* at 25°C, the order of magnitude is reasonable. Positive feedback, not modeled here, in the LuxI/LuxR circuit would presumably tend to accelerate AI production as the concentration increases, and this would reduce the apparent value of  $\tau$ . We can use the fit result to estimate the basal rate of AI production by the (noninduced) cell: If the threshold concentration of AI is of order  $C^* \sim 50$  nM, we expect an AI production rate  $k \sim C^*/(2,600 \text{ min/pl}) \sim 2 \times 10^{-23}$  M/min  $\sim 10$  molecules/min. If the typical noninduced cell contains  $\sim 10$  LuxI molecules, this estimate for  $k$  is reasonably consistent with literature data that indicate that a single molecule of LuxI synthesizes  $\sim 1$  molecule of AI per minute [12, 18]. This estimate of 10 LuxI molecules is also consistent with the observed 20–30% variations in  $t^*$ , as discussed above. Only additional experiments can confirm these estimates, however.

The logarithmic dependence of  $t^*$  on the chamber volume suggests that the LuxI/LuxR circuit senses the local volume very poorly. In order for the onset time  $t^*$  to become linear in  $V$ , and therefore more sensitive to chamber volume, the chamber would have to be small enough that the basal AI production could trigger autoinduction before the cells have grown appreciably. Equation 2 suggests that this requires extremely small chambers, with  $V \ll k\tau/C^* \sim 10$  fl, i.e., chambers no larger than  $\sim 2 \times 2 \times 2 \mu\text{m}^3$ . Autoinduction would then occur (given Eq. 2) in a time  $t^* \sim VC^*/k = 26$  min. Although it is presumably possible to confine a single cell within a volume of this size, this experiment quickly reaches a practical limit, as the volume of the *E. coli* cell itself is only  $\sim 1$  fl [19]. In this sense, the QS circuit becomes a sensitive probe of the confinement volume only in the extreme case of a cell packed within a tight space. In that case, however, one expects that the same noise that generates variability in  $t^*$  here would complicate the use of  $t^*$  as a probe of chamber volume.

## 5 Conclusions

Confinement of individual cells of *V. fischeri* to microscopic chambers does lead to induction of the *lux* bioluminescence genes, although the weak bioluminescence emission and the high motility of the cells make it difficult to perform a quantitative study. Using an *E. coli* strain in which the LuxI/LuxR QS circuit of *V. fischeri* regulates *gfp* expression, we were able to trigger autoinduction by confinement in closed, microscopic chambers. Autoinduction occurs at  $\sim 100$ – $200$  min in chambers of  $\sim 3$ – $18$ -pl volume, although autoinduction time varies dramatically between cells. The consequences of this variability would presumably be minimal in larger populations and in larger volumes, but the effect is pronounced at the level of individual cells and small clusters. Variability between individual cells is expected to arise from stochasticity in the QS regulatory network [12]; interestingly, it has a greater effect on the rate of autoinduction than does the volume of the confining chamber. Hence, our results suggest that the exponential growth of the cells tends to reduce the sensitivity of the QS circuit to the volume of the local microenvironment. Of course, it is possible that QS pathways in other species provide a less noisy volume-sensing function; *V. fischeri* may not have acquired a particularly sensitive one because it does not require

one in its biological niche. On the other hand, it is interesting that the concurrence of auto-induction and growth means that gene expression is primarily synchronized among common daughters of the parent cell. The potential for DS in the presence of stochastic gene expression will be an interesting area for future study.

**Acknowledgements** The authors thank Drs. Mark Mandel, Ned Ruby, Rena Hill, and Christopher Voigt for providing bacterial strains used in this study. The authors also gratefully acknowledge funding support from the National Science Foundation MCB no. 0347124 and the National Institutes of Health NIDCR 1R21DE018826.

## References

1. Waters, C.M., Bassler, B.L.: Quorum sensing: cell-to-cell communication in bacteria. *Annu. Rev. Cell Dev. Biol.* **21**, 319–346 (2005)
2. Boyer, M., Wisniewski-Dye, F.: Cell-cell signalling in bacteria: not simply a matter of quorum. *FEMS Microbiol. Ecol.* **70**, 1–19 (2009)
3. Dunn, A.K., Stabb, E.V.: Beyond quorum sensing: the complexities of prokaryotic parliamentary procedures. *Anal. Bioanal. Chem.* **387**, 391–398 (2007)
4. Hense, B.A., Kuttler, C., Mueller, J., Rothballer, M., Hartmann, A., Kreft, J.: Does efficiency sensing unify diffusion and quorum sensing? *Nat. Rev. Microbiol.* **5**, 230–239 (2007)
5. Redfield, R.J.: Is quorum sensing a side effect of diffusion sensing? *Trends Microbiol.* **10**, 365–370 (2002)
6. Dunlap, P.V.: Quorum regulation of luminescence in *Vibrio fischeri*. *J. Mol. Microbiol. Biotechnol.* **1**, 5–12 (1999)
7. Lupp, C., Urbanowski, M., Greenberg, E.P., Ruby, E.G.: The *Vibrio fischeri* quorum-sensing systems *ain* and *lux* sequentially induce luminescence gene expression and are important for persistence in the squid host. *Mol. Microbiol.* **50**, 319–331 (2003)
8. You, L.C., Cox, R.S., Weiss, R., Arnold, F.H.: Programmed population control by cell-cell communication and regulated killing. *Nature* **428**, 868–871 (2004)
9. March, J.C., Bentley, W.E.: Quorum sensing and bacterial cross-talk in biotechnology. *Curr. Opin. Biotechnol.* **15**, 495–502 (2004)
10. James, S., Nilsson, P., James, G., Kjelleberg, S., Fagerstrom, T.: Luminescence control in the marine bacterium *Vibrio fischeri*: an analysis of the dynamics of *lux* regulation. *J. Mol. Biol.* **296**, 1127–1137 (2000)
11. Zhou, T.S., Chen, L.N., Aihara, K.: Molecular communication through stochastic synchronization induced by extracellular fluctuations. *Phys. Rev. Lett.* **95**, 178103 (2005)
12. Cox, C.D., Peterson, G.D., Allen, M.S., Lancaster, J.M., McCollum, J.M., Austin, D., Yan, L., Saylor, G.S., Simpson, M.L.: Analysis of noise in quorum sensing. *OMICS: A J. Integr. Biol.* **7**, 317–334 (2003)
13. Sia, S.K., Whitesides, G.M.: Microfluidic devices fabricated in poly(dimethylsiloxane) for biological studies. *Electrophoresis* **24**, 3563–3576 (2003)
14. Eberhard, A.: Inhibition and activation of bacterial luciferase synthesis. *J. Bacteriol.* **109**, 1101 (1972)
15. Anderson, J.C., Clarke, E.J., Arkin, A.P., Voigt, C.A.: Environmentally controlled invasion of cancer cells by engineered bacteria. *J. Mol. Biol.* **355**, 619–627 (2006)
16. Boedicker, J.Q., Vincent, M.E., Ismagilov, R.F.: Microfluidic confinement of single cells of bacteria in small volumes initiates high-density behavior of quorum sensing and growth and reveals its variability. *Angew. Chem. Int. Ed.* **48**, 5908–5911 (2009)
17. Carnes, E.C., Lopez, D.M., Donegan, N.P., Cheung, A., Gresham, H., Timmins, G.S., Brinker, C.J.: Confinement-induced quorum sensing of individual *Staphylococcus aureus* bacteria. *Nat. Chem. Biol.* **6**, 41–45 (2010)
18. Schaefer, A.L., Val, D.L., Hanzelka, B.L., Cronan, J.E., Greenberg, E.P.: Generation of cell-to-cell signals in quorum sensing: Acyl homoserine lactone synthase activity of a purified *Vibrio fischeri* LuxI protein. *Proc. Natl. Acad. Sci. U. S. A.* **93**, 9505–9509 (1996)
19. Kubitschek, H.E., Friske, J.A.: Determination of bacterial cell volume with the Coulter Counter. *J. Bacteriol.* **168**, 1466–1467 (1986)